

## Automatic visual inspection for silica caps

Ahmed Osama<sup>1</sup>, Alaa Hamdy<sup>2</sup>, Sameh Salem<sup>3</sup>

1(Dept. Communication & Electronics, Helwan University/Engineering, and Cairo/Egypt)

2(Dept. Communication & Electronics, Helwan University/Engineering, and Cairo/Egypt)

3(Dept. Communication & Electronics, Helwan University/Engineering, and Cairo/Egypt)

### Abstract:

In this paper, an automatic visual inspection system for checking silica caps is proposed. The proposed system is able to inspect silica cap and detect outer ring and inner cap defects. This variability is managed in an automatic way by means of using reject piston to automatically reject defects. Furthermore, the system is coupled to install the product on a conveyor to achieve inspection process without affecting the production act time. To achieve a robust inspection process, two algorithms are introduced; the first is a segmentation algorithm for extracting outer ring from images, while second is a recognition algorithm for inner cap inspection. Experimental results on different lots of real production show the robustness and reliability of the proposed in inspecting the silica caps.

*Keywords* — inspection for silica caps Automated

### I. INTRODUCTION

For decades, automatic visual inspection represented a cornerstone in the field of quality control [1-3]. Computer vision algorithms as applied to the industrial production environment can be used to perform complex quality controls and achieve lower cost in production.

These systems are important in complete stepwise checking of the produced items instead of sampling along the production batch. For instance, visual inspection is highly critical in semiconductor production [4-5]. Interestingly, automatic visual inspection is a clean, non-invasive process that could be successfully employed in various industrial processes [6-7]. A wide range of sensors could be exhibited in an automatic visual inspection such as near infrared cameras, far infrared cameras [8-10], X-ray cameras [11], or even ultrasound imaging [12].

In this research, a system for inspecting silica caps manufacturing defects is proposed. The system was integrated into a camera, florescent lamp, belt conveyor, reject defect piston and inspection

Silica caps which are transported on a movable belt conveyor and give order to defect reject piston to make reject for any defect as shown in Fig. 1.

The paper is organized as follows: in Section II related works are revised and relevant algorithms and systems are analysed to understand similarities and differences with our system. In Section III the proposed system is described, including hardware setup, design principles and user interface. In Section IV the image analysis algorithms proposed for solving the discussed visual inspection problem are described in detail; this includes wire identification and color indexing. In Section V experiments run for assessing the system performance in terms of detection accuracy, true positive rate and computational load are discussed, and their outcomes are reported. Finally, in Section VI a summary of the work done is reported, together with some final remarks.

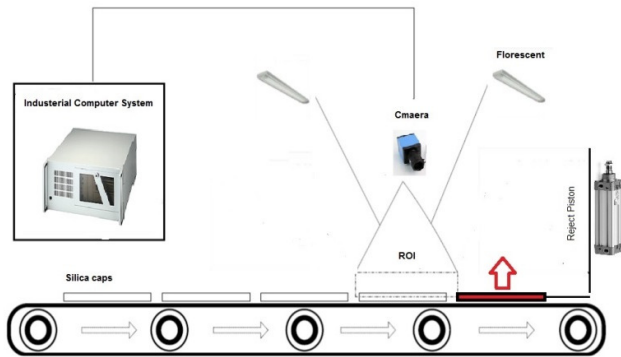


Fig. 1 System for inspecting silica caps manufacturing defects.

## II. RELATED WORK

Visual inspection represents a key player in industrial production, involving food, medical and fabric productions [7, 13-14]. Establishing computer vision techniques has proven to be successful; however these techniques require accurate hardware and setup selection [15-16]. In addition to the capability of being real time i.e. being able to check the production without affecting the production process speed [17].

From this perspective, Observation is easy to know the similarity between visual inspection systems and robotic vision systems in its ability in data extraction and sampling from the environment in real time for robots to execute the most suitable action.

Color information analysis is extensively used in computer vision and its applications, including visual inspection [18-19]. Although sophisticated techniques for handling color information also exist in the literature [21], color indexing is often expressed by histograms [20], which are considered as one of the suitable techniques of managing color information and creating clusters of similar colors. Moments of color distributions are considered, while color signature based on bag of colors are presented in [22]; color itself can be described in a number of different color spaces, that can ease the task of discriminating one from another [23]. The previously mentioned techniques were mainly developed to work on real-world scenes, similar to robotics and computervision applications like video surveillance or object recognition.

## III. SYSTEM DESCRIPTION

Visual inspection needs to be performed just after manufacturing of silica cap finished, while they are being guided out of manufacturing process. Thus the quality inspection is needed for checking for defects.

### A. System requirements

The goal of the inspection system is to check whether silica cap's outer ring is good and its inner color order. All produced items must be checked by an inspection system that could be able to keep up with the tact time. Therefore, the computer vision algorithm should run in a time slot shorter than the cycle time, depending on the number of silica cap produced by the machine.

Silica cap are composed of an inner cap and an outer ring (Fig. 2), and their defects mainly occur in each part separately.

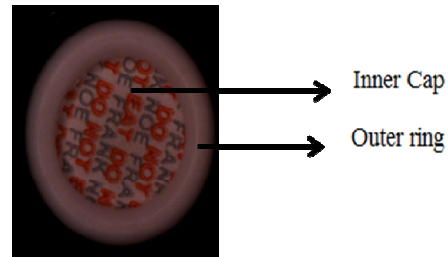


Fig. 2 Silica cap

### B. Vision system

The vision system is composed of a camera, a florescent lamp, industrial computer system and a reject piston, as shown in figure 1. It is installed on the belt conveyor, as it can be seen in figure 1. In industrial visual inspection light control is very common, and lighting is therefore part of the system itself [24-25]. Choices made at this stage strongly influence the image quality and thus the system performance, and should be made in order to minimize the noise sources. In the final setup the lighting system is fixed on the front face of the belt conveyor, at a height of 120mm to the working plane of our inspection system.

All of photos which in this paper is first time to use and it's took using industrial cam which give image information (Width: 658 pixels, Height: 492 pixels and Bit depth: 24).

C. Color-learning system

During the learning phase, tolerances in color definition are tuned. Learning starts using two sets of threshold triplets, (ThL) and (ThH), to be applied on the H, S and V values of Inner cap color. The former set represents a strong constraint, and is employed to verify whether two colors are the same with high confidence: (H1;S1;V1) and (H2;S2;V2) are considered to be equal if:

$$\{ |H1 - H2| < ThL:H \text{ and } |S1 - S2| < ThL:S \text{ and } |V1 - V2| < ThL:V \}$$
 (1)

By this way a low tolerance is obtained, i.e. two colors are considered to be equal only if the differences in their H, S and V values are very small. The second set of thresholds leads to a higher tolerance. When the colors of two Inner cap are compared, the same color are automatically considered if their difference satisfies (1), and the different color are automatically considered if such difference exceeds {ThH}, that is:

$$\{ |H1 - H2| > ThH:H \text{ and } |S1 - S2| > ThH:S \text{ and } |V1 - V2| > ThH:V \}$$
 (2)

When the color comparison does not satisfy (1) nor (2). The operator is asked if the two colors should be considered the same or not. This check is performed only once observing the Inner cap: in other words, the system prompts the users if some caps show colors that are similar, but do not look exactly the same.

D. User Interface

System provides a graphical user interface (GUI), carefully designed to ease the communication with interface board which is connected with PLC that takes action to accept or reject set through reject piston. At the beginning of a new production, the GUI starts and silica caps pass under the camera. If a silica cap doesn't have any defects, it will pass and light green lamp on the screen but if i has any defect it will light red lamp and reject signal will order the piston to reject this set which is collected in defect box .Then, the conveyor moves to make inspection for next set.

All the software for visual inspection has been developed in LabVIEW and is based on the

LabVIEW library for data structures and classes, color conversion and image processing algorithms. The software modules described in the following have been written by the authors from scratch using LabVIEW image processing functions.

IV. VISUAL INSPECTION ALGORITHM

Visual inspection process divided in two parts which is outer inspection and inner inspection as shown in Fig. 3.

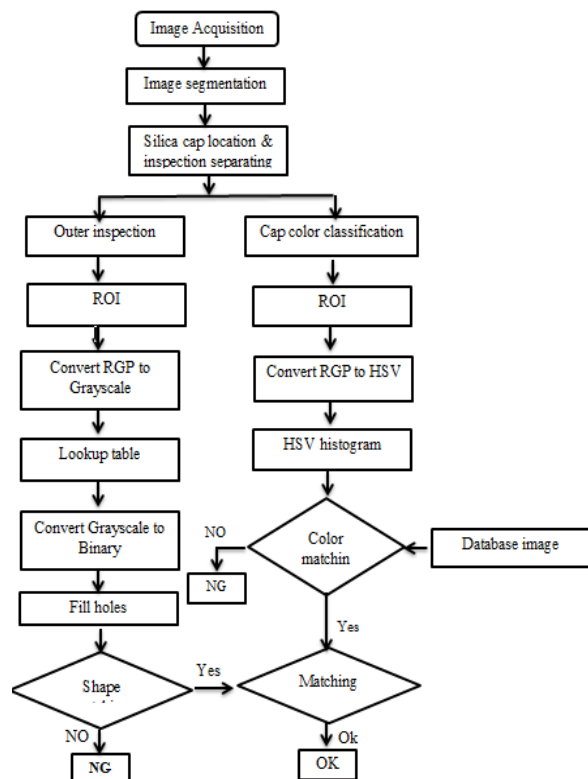


Fig. 3 An overview of the whole inspection.

A. Outer Ring inspection

- 1) ROI: Outer ring inspection performed started with by set image mask on neglected as preparation for made image subtraction to detect area which needed toinspect.
- 2) Second step made convert RGB image to grayscale through equation:

$$Y = 0.299R + 0.587G + 0.114B$$
 (3)

- 3) Lookup table: Adjust brightness and contrast values using functions from (4 – 12), The histogram function H(k) is simply defined as

$$H(k) = nk$$
 (4)

Then our function  $f(g)$  will modify the gray-level values according to

$$Sout(x, y) = f(Sin(x, y)) \quad (5)$$

With  $sin$  as the original values and  $sout$  as the resulting values. Because the possible results are limited to 256 values, the function  $f(g)$  usually is realized by a table consisting of 256 values, a look-up table (LuT). Therefore, if

$$LuT(g) = f(g) \quad (6)$$

$$sout(x, y) = LuT(Sin(x, y)) \quad (7)$$

The logarithm (base 10) of 255 is about 2.4, so have to scale the entire range of resulting values to the 8-bit grayscale set. The resulting function is

$$Sout(x, y) = \log(Sin(x, y)) \cdot 255 / (\log(255)) \\ = \log(Sin(x, y)) \cdot 105.96 \quad (8)$$

The next function is exponential. If it's generated the way did above, it's found a far too step function because the values rise too fast. A correction factor  $c$ , according to

$$Sout(x, y) = \exp(Sin(x, y) / c) \cdot 255 / (\log(255 / c)) \quad (9)$$

leads to more reasonable results.  $c \approx 48$  is the value used in the built-in IMAQ function. The square function is easy: If made multiply the value location by itself and scale it like that did above, so that get

$$Sout(x, y) = (Sin(x, y))^2 \cdot 255 / (255)^2 \\ = (Sin(x, y))^2 \cdot 1 / 255 \quad (10)$$

$$Sout(x, y) = \sqrt{Sin(x, y)} \cdot \frac{255}{\sqrt{255}} \approx$$

$$Sout(x, y) = \sqrt{Sin(x, y) \cdot 255} / \sqrt{255} \quad (11)$$

The next two cases need an additional factor called power value  $p$ : below function is created

$$Sout(x, y) = (Sin(x, y))^P \cdot 255 / (255)^P \\ = (Sin(x, y))^P \cdot 1 / (255)^{P-1} \quad (12)$$

4) Convert image from grayscale to binary: with threshold (0~ 26).

5) Fill hole: using morphological operation.

6) Shape matching: Perform a shape matching using image subtraction. The outer ring inspection process is summarized in Algorithm shown in Fig. 4.

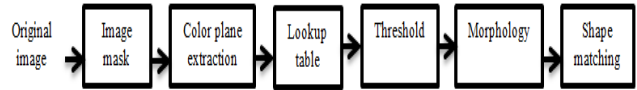


Fig. 4 A Summary of outer ring inspection process.

### B. Inner Color inspection

1) *Image Mask*: Inner inspection performed started with by making ROI (region of interest) to select the target area.

2) *Convert RGB image to HSV image*: by using below formula from (13 – 18) to correct uneven illumination in the area framed by the visual inspection machine. In order to reduce noise. The filtered image is then transformed into the HSV (Hue Saturation Value) color space, and the average values for the saturation and value channels are calculated. For each background pixel the S and V channels are compared to the average, in order to understand whether it is lighter or darker the difference calculated for each pixel is used to obtain an equalized image before the actual inspection process takes place. Information gathered at this stage will be used to correct pixel by pixel each acquired image before the actual inspection process takes place.

$$R' = R / 255 \quad (13)$$

$$G' = G / 255 \quad (14)$$

$$B' = B / 255 \quad (15)$$

$$C_{max} = \max(R', G', B') \quad (16)$$

$$C_{min} = \min(R', G', B') \quad (17)$$

$$\Delta = C_{max} - C_{min} \quad (18)$$

Hue calculation as in (19):

$$H = \begin{cases} 0^\circ & \Delta = 0 \\ 60^\circ \times \left( \frac{G' - B'}{\Delta} \text{ mod } 6 \right), & C_{max} = R' \\ 60^\circ \times \left( \frac{B' - R'}{\Delta} + 2 \right), & C_{max} = G' \\ 60^\circ \times \left( \frac{R' - G'}{\Delta} + 4 \right), & C_{max} = B' \end{cases} \quad (19)$$

Saturation calculation as in (20):

$$S = \begin{cases} 0 & , C_{max} \neq 0 \\ \frac{\Delta}{C_{max}} & , C_{max} \neq 0 \end{cases} \quad (20)$$

Value calculation as in (21):

$$V=C\_max \quad (21)$$

RGB to HSV color table as shown in Fig. 5.

Color	Color name	Hex	(R,G,B)	(H,S,V)
Black	Black	#000000	(0,0,0)	(0°,0%,0%)
White	White	#FFFFFF	(255,255,255)	(0°,0%,100%)
Red	Red	#FF0000	(255,0,0)	(0°,100%,100%)
Lime	Lime	#00FF00	(0,255,0)	(120°,100%,100%)
Blue	Blue	#0000FF	(0,0,255)	(240°,100%,100%)
Yellow	Yellow	#FFFF00	(255,255,0)	(60°,100%,100%)
Cyan	Cyan	#00FFFF	(0,255,255)	(180°,100%,100%)
Magenta	Magenta	#FF00FF	(255,0,255)	(300°,100%,100%)
Silver	Silver	#C0C0C0	(192,192,192)	(0°,0%,75%)
Gray	Gray	#808080	(128,128,128)	(0°,0%,50%)
Maroon	Maroon	#800000	(128,0,0)	(0°,100%,50%)
Olive	Olive	#808000	(128,128,0)	(60°,100%,50%)
Green	Green	#008000	(0,128,0)	(120°,100%,50%)
Purple	Purple	#800080	(128,0,128)	(300°,100%,50%)
Teal	Teal	#008080	(0,128,128)	(180°,100%,50%)
Navy	Navy	#000080	(0,0,128)	(240°,100%,50%)

Fig. 5 RGB to HSV color table

3) Program color training: Learning starts using two sets of threshold triplets, (ThL) and (ThH), the training is performed by taking some accepted samples to calculate its HSV using an accepted degree of tolerance to be used as an accepted degree. On the other hand, some rejected samples used to calculate its HSV degree using tolerance to be used as a degree of reject.

The Inner inspection process is summarized in Algorithm shown in Fig. 6.



Fig. 6 A Summary of inner inspection process

## V. EXPERIMENTAL RESULTS

The quality inspection system, installed on production line, has been tested on real production images. Tests involved several different caps lots, caps used in our experiments were taken from several production lots, each lot contains several types of defects. Our system can detect all of these defects as shown in below.

### A. First defect part (outer ring):

1) The top-view image for a defect in outer ring shown in Fig.7.



Fig.7 Top-view image for defect in outer ring

2) The inspection process for outer ring output shown in Fig. 8.



Fig. 8A Outer ring ROI



Fig.8B RGB image conversion to grayscale



Fig.8C Brightness and Contrast values Adjustment



Fig. 8D Image conversion from grayscale to binary

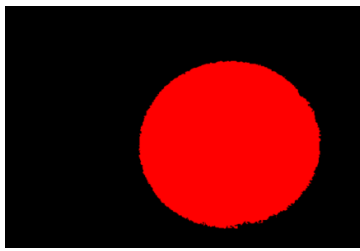


Fig.8E Fill hole formation

**B. Second defect part (Inner Cap).**

1) Top-view image of a defect types in Inner cap shown in Fig. 9.



Fig.9 Top-view image of a defect in Inner cap

2) The inspection process for outer ring output shown in Fig. 10.

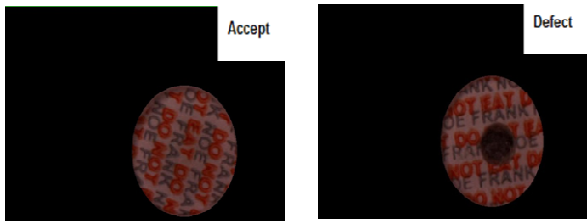


Fig.10A Selection of target area requiring inspection.



Fig.10B HSV histogram for Accepted and defected sample

System is providing graphical user interface to be easy for production member to use the system and follow inspection process as shown in Fig 11.

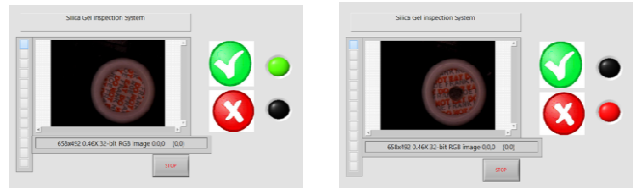


Fig.11 A graphical user interface (GUI)

System test all types of defects which detect before from production side and result show in below table

TABLE I INSPECTION SYSTEM TEST RESULT

Defect	Defects Numbers	System Detection	Result
Outer ring	3	3	100%
Inner cap	4	4	100%

**VI. CONCLUSIONS**

In this paper, a system for automatic visual inspection for production of silica caps has been introduced. The inspection system has been installed into a production conveyor, and tested on a series of real production images. The main sources of defects come from two main factors: strong noise on the observed caps that make it almost impossible to precisely recognize the inner color, and the uneven illumination conditions. While the former depends on the raw materials used in the production, the latter effect can be eliminated with a larger observation window, and a stronger illumination. Both could be achieved if closed environmental design is occurred to host the visual inspection system, leaving more room for placing the hardware. The limitations in the current version are due to the fact that the region which is selected to install system mustn't be modified and thus the visual inspection hardware had to be installed in a small fixed empty region.

## REFERENCES

1. T. Newman and A. Jain, "A survey of automated visual inspection," *Computer vision and image understanding*, vol. 61, no. 2, pp. 231–262, 1995.
2. E. Malamas, E. Petrakis, M. Zervakis, L. Petit, and J.-D. Legat, "A survey on industrial vision systems, applications and tools," *Image and vision computing*, vol. 21, no. 2, pp. 171–188, 2003.
3. M. Shirvaikar, "Trends in automated visual inspection," *Journal of Real-Time Image Processing*, vol. 1, no. 1, pp. 41–43, 2006.
4. E Guerra and J. Villalobos, "A three-dimensional automated visual inspection system for smt assembly," *Computers & industrial engineering*, vol. 40, no. 1, pp. 175–190, 2001.
5. X. Lu, G. Liao, Z. Zha, Q. Xia, and T. Shi, "A novel approach for flip chip solder joint inspection based on pulsed phase thermography," *NDT & E International*, vol. 44, no. 6, pp. 484–489, 2011.
6. Suresh, R. Fundakowski, T. Levitt, and J. Overland, "A real-time automated visual inspection system for hot steel slabs," *Pattern Analysis and Machine Intelligence, IEEE Transactions on*, vol. 5, no. 6, pp. 563–572, 1983.
7. G. Moreda, J. Ortiz-Cañavate, F. García-Ramos, and M. Ruiz-Altisent, "Non-destructive technologies for fruit and vegetable size determination A review," *Journal of Food Engineering*, vol. 92, no. 2, pp. 119–136, May 2009.
8. M. S. Millán and J. Escofet, "Fabric inspection by near-infrared machine vision," *Optics Letters*, vol. 29, no. 13, pp. 1440–1442, Jul 2004.
9. S. Ghidoni, M. Minella, L. Nanni, C. Ferrari, M. Moro, E. Pagello, and E. Menegatti, "Automatic crack detection in thermal images for metal parts," in *Heating by Electromagnetic Sources, Proceedings of the International conference on*, May 2013.
10. T. Ummerhofer and J. Medgenberg, "On the use of infrared thermography for the analysis of fatigue damage processes in welded joints," *International Journal of Fatigue*, vol. 31, no. 1, pp. 130–137, 2009.
11. Neubauer, "Intelligent x-ray inspection for quality control of solder joints," *Components, Packaging, and Manufacturing Technology, Part C, IEEE Transactions on*, vol. 20, no. 2, pp. 111–120, 1997.
12. Jiang, C.-C. Wang, H.-J. Chen, and C.-C. Chu, "Automatic bubble defect inspection for microwave communication substrates using multithreshold technique based co-occurrence matrix," *International Journal of Production Research*, vol. 48, no. 8, pp. 2361–2371, 2010.
13. R. Ureña, F. Rodríguez, and M. Berenguel, "A machine vision system for seeds quality evaluation using fuzzy logic," *Computers and Electronics in Agriculture*, vol. 32, no. 1, pp. 1–20, 2001.
14. J. Jia, "A Machine Vision Application for Industrial Assembly Inspection," in *ICMV '09. Second International Conference on Machine Vision, 2009. Ieee, Dec. 2009*, pp. 172–176.

15. Shumin, L. Zhoufeng, and L. Chunlei, "Adaboost learning for fabric defect detection based on hog and svm," in International Conference on Multimedia Technology (ICMT), 2011, no. 1. IEEE, Jul. 2011, pp. 2903–2906.
16. Kumar and K. Kannan, "A Roadmap for Designing an Automated Visual Inspection System," International Journal of Computer Applications, vol. 1, no. 19, pp. 34–37, 2010.
17. M. Rajeswari and M. Rodd, "Real-time analysis of an IC wire-bonding inspection system," Real-Time Imaging, vol. 5, no. 6, pp. 409–421, 1999.
18. H.-H. Wu, X.-M. Zhang, and S.-L. Hong, "A visual inspection system for surface mounted components based on color features," in International Conference on Information and Automation, 2009. ICIA'09. IEEE, Jun. 2009, pp. 571–576.
19. J. Derganc, B. Likar, R. Bernard, D. Tomaževič, and F. Pernuš, "Realtime automated visual inspection of color tablets in pharmaceutical blisters," Real-Time Imaging, vol. 9, no. 2, pp. 113–124, Apr. 2003.
20. M. Swain and D. Ballard, "Color indexing," International journal of computer vision, vol. 7, no. 1, pp. 11–32, 1991.
21. Z.-C. Huang, P. Chan, W. Ng, and D. Yeung, "Content-based image retrieval using color moment and gabor texture feature," in Machine Learning and Cybernetics (ICMLC), 2010 International Conference on, vol. 2. IEEE, 2010, pp. 719–724.
22. C. Wengert, M. Douze, and H. Jégou, "Bag-of-colors for improved image search," in Proceedings of the 19th ACM international conference on Multimedia. ACM, 2011, pp. 1437–1440.
23. J. Yang, C. Liu, and L. Zhang, "Color space normalization: Enhancing the discriminating power of color spaces for face recognition," Pattern Recognition, vol. 43, no. 4, pp. 1454–1466, 2010.
24. A. Thomas, M. Rodd, J. Holt, and C. Neill, "Real-time industrial visual inspection: A review," Real-Time Imaging, vol. 1, no. 2, pp. 139–158, 1995.
25. C.-S. Cho, B.-M. Chung, and M.-J. Park, "Development of real-time vision-based fabric inspection system," Industrial Electronics, IEEE Transactions on, vol. 52, no. 4, pp. 1073–1079, 2005.